Desalination and Water Treatment
www.deswater.com
doi: 10.5004/dwt.2023.29406

289 (2023) 155–162
March

Synthesis of N-doped TiO_2 nanoparticle and its application for disinfection of a treatment plant effluent from hospital wastewater

Hossein Kamani[a], Seyed Davoud Ashrafi[a], Eder C. Lima[c], Ayat Hossein Panahi[d,*], Mahdieh Garkani Nezhad[a,*], Hossein Abdipour[d]

[a]*Health Promotion Research Center, Zahedan University of Medical Sciences, Zahedan, Iran, Tel.: +989136110638; emails: M.g.3179921080@gmail.com (M.G. Nezhad), Hossein_kamani@yahoo.com (H. Kamani)*
[b]*Department of Environmental Health Engineering, Research Center of Health and Environment, School of Health, Guilan University of Medical Sciences, Rasht, Iran, email: d.ashrafi@yahoo.com*
[c]*Institute of Chemistry-Federal University of Rio Grande do Sul (UFRGS), Porto Alegre, RS, Brazil, email: profederlima@gmail.com*
[d]*Student Research Committee, Department of Environmental Health Engineering, Hamadan University of Medical Sciences, Hamadan, Iran, Tel.: +989378657378; emails: ayatpanahi@yahoo.com (A. Hossein Panahi), Abdypour95@gmail.com (H. Abdipour)*

Received 17 April 2022; Accepted 17 February 2023

ABSTRACT

Disinfection is one of the most important stages of water and wastewater treatment. Today, the use of photocatalytic processes by sunlight as a sustainable way of water disinfection has been noted. The purpose of this study was to remove coliform and fecal coliform from the effluent of a hospital sewage treatment plant using the solar/N-doped titanium dioxide (TiO_2) process. In order to conduct the experiments, the raw samples (effluent of secondary sedimentation) were taken from the Ali Ibn Abi Talib hospital wastewater treatment plant in Zahedan City, Iran. N-doped TiO_2 nanoparticles and the samples were poured into the reactor and then exposed to direct sunlight in summer. The results indicated that the photocatalytic process efficiency was enhanced by increasing reaction time and nanoparticles dosage. Furthermore, it was found that N-doped TiO_2 nanoparticles and sunlight had a synergistic effect on the deactivation of coliform and fecal coliform. The number of coliforms and fecal coliforms bacteria cells decreased from 5×10^5 to 7×10^3 MPN/100 mL and 4×10^3 to 2×10^2 MPN/100 mL in the solar/N-doped TiO_2 process after 150 min, respectively. It has been generally concluded that the solar/N-doped TiO_2 process can effectively deactivate a wide range of real effluent microorganisms on a laboratory scale.

Keywords: Coliform; Fecal coliform; N-doped titanium dioxide; Disinfection; Synthesis

1. Introduction

According to the United Nations, two-thirds of the world's population now live in areas where water shortages are at least once a month. Therefore, providing drinking water for these areas is the main priority in those countries [1]. Many countries have sought to supply fresh water from unconventional sources, including desalination, rainwater harvesting, sewage treatment, and lukewarm water. In the meantime, wastewater treatment can help the water crisis and tension by preventing the pollution of surface and underground water sources [2]. Hospital wastewaters include disinfectants, detergents, contagious/stool disposal, intestinal pathogens, bacteria, viruses, helmets, drugs, and chemicals. Therefore, it is expected that a wide range of bacteria and viruses in the effluent from the activated sludge process [3]. These substances are recognized by World Health Organization as hazardous compounds and must be removed before reaching water sources. Some strategies have been implemented to develop sustainable wastewater

* Corresponding authors.

treatment technologies, such as chlorination, ultraviolet radiation, ozonation, and advanced oxidation processes (AOPs) [4–8]. The results of studies indicated that direct oxidation by ROS (reactive oxygen species) are the major pathway responsible for organic matter degradation, but they are not very effective in a suspension medium. AOPs such as the photocatalytic process by producing hydroxyl radical ($OH^{\bullet}$) and active, positive holes (h^{+}) have received much attention [9–11]. The process has been widely used to advance wastewater treatment. Among the photocatalysts, titanium dioxide (TiO_2) has received more attention than other semiconductor photocatalysts because of their good photocatalytic properties [12–14]. TiO_2 is a non-toxic chemical, water-insoluble, resistant to UV, and relatively inexpensive [15,16]. The efficiency of the photocatalytic process is not influenced only by the nature of the photocatalyst used, but the factors such as catalyst dosage, light intensity, temperature, and pH also can have significant effects on its performance [13]. Studies have shown that modifying the surface of nanoparticles by a ligand or other elements can effectively improve photocatalytic activity. Nitrogen is one such compound used for modification [17–19]. This study aimed to evaluate the photocatalytic degradation for disinfection of wastewater treatment effluent by N-doped TiO_2 under sunlight irradiation.

2. Material and methods

2.1. Synthesis of N-doped TiO_2

A sol–gel method was used to synthesize N-doped TiO_2 nanoparticles. To prepare N-doped TiO_2 by molar ratio doping of 3%, 6%, and 12%, 3 mL titanium isopropoxide and 2 mL (TN1), 4 mL (TN2), and 8 mL (TN2) of triethylamine were dissolved in 20 mL of EtOH, then was stirred for 15 min (sample A). Subsequently, 2 mL of H_2O was added to 10 mL of EtOH that contained HNO_3. Next, the sample obtained was stirred during 15 min (sample B). Next, sample B was added dropwise to sample A, along with magnetic stirring. After a half-hour of stirring, the sol (semi-transparent) was acquired. Next, the sol was placed at room temperature for 5 h and then dried in an oven at 80°C for 24 h. Finally, the achieved powder was calcinated in an electric furnace at 500°C for 60 min at 16°C/min. Non-doped TiO_2 sample was also fabricated without adding the triethylamine using exactly the same experimental conditions to compare the presence and absence of the dopant.

2.2. Characterization of photocatalyst

The X-ray diffraction (XRD) diffractograms were obtained using an X-ray Diffractometer (Philips X'Pert, Made from Netherlands) with 2θ in the range of 10°–70°, using Cu Kα radiation. The Scherrer equation was utilized to calculate the average crystallite size.

The surface morphology, structure, and shape of N-doped TiO_2 nanoparticles were achieved using a field-emission scanning electron microscopy (FE-SEM).

2.3. Wastewater samples and their properties

Non-chlorinated secondary effluent was taken from the secondary clarifiers at the Ali Ibn Abi Talib hospital wastewater treatment plant in Zahedan City, Iran. The type of process in the treatment plant was extended aeration-activated sludge (Fig. 1). The samples were stored at 4°C and used within 1 d. Real wastewater samples (required: 50 L) were taken from a secondary settling effluent of a biological treatment process. Biochemical oxygen demand (BOD_5), chemical oxygen demand (COD), pH, total suspended solids (TSS), electrical conductivity (EC), and turbidity of raw samples were measured and recorded. The Iranian Department of the Environment (DoE) considers these parameters significant factors for monitoring and evaluating wastewater treatment. The sample was analyzed according to the standard methods [20]. All the analyses were conducted in the water and wastewater laboratory at the department of environmental health at Zahedan University of Medical Sciences. The mean of BOD_5, COD, TSS, pH, EC, and turbidity is reported in Table 1.

2.4. Light source and reactor

The efficiency of the photocatalytic process using N-doped TiO_2 was evaluated in the removal of coliform and fecal coliform bacteria. The samples were placed under sunlight irradiation in the suspended photocatalyst's presence. The reactor was a glass container with length, width, and height equal to 100, 50, and 30 cm, respectively. One mixer was installed in the reactor to homogenize and suspend reactor contents. The experiments were conducted under summer midday sunlight in Zahedan City to confirm and ensure the maximum presence of light and solar photocatalytic activity. The temperature during experiments was maintained at 21°C ± 4°C by a water cooling system and a thermometer. The graphical schematic of the reactor is shown in Fig. 2.

2.5. Photocatalytic experiments

The pH of the solutions was adjusted to the desired level using hydrochloric acid (HCl, M = 36.45 g/mol, Purity = fuming 37%) and sodium hydroxide (NaOH, M = 40.0 g/mol, Purity = 100%) as well as the pH-meter (model: MTT65). The reactor was filled with 5 L of effluent, and after adjusting the parameters, nanoparticles were added to it, then placed under sunlight irradiation for over 150 min. In the tests, the effect of various parameters such as time (60.120 and 150 min), visible light and darkness, and N-doped TiO_2 (120 and 180 mg/L) were investigated on the efficiency of photocatalytic activity. All experiments were performed at constant temperature (21°C ± 2°C). 10 mL of the mixed liquid in each test was drawn at different times (60, 120, and 150 min) and immediately shed with 0.9% saline. 1 mL of each dilution was inoculated with lactose and maintained for 48 h at 37°C. Finally, by a sterile loop, two drops of the positive samples in the presumptive test were inoculated into Lactose Broth and BGB and placed at 37°C and 44°C, respectively. Gas production in the Durham tube indicated a positive microbial test. Before and after photocatalytic tests, the most probable number (MPN/100 mL) of total coliform and fecal coliform bacteria in samples was measured. The entire experiments were repeated twice, and their average values were reported. The disinfection efficiency, E, is calculated as follows [Eq. (1)]:

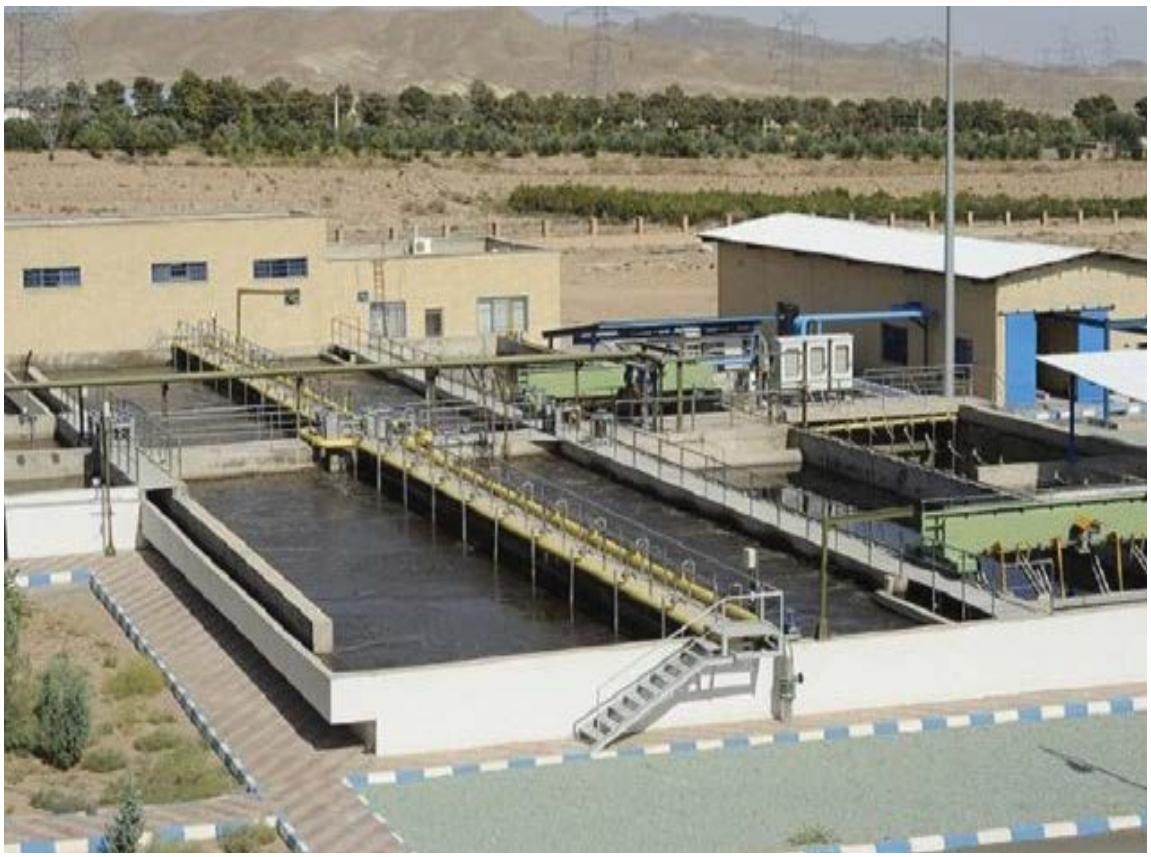

Fig. 1. Ali Ibn Abi Talib hospital wastewater treatment plant in Zahedan City, Iran.

Table 1
Physico-chemical and microbiological characterization of the effluent of the hospital wastewater treatment plant

Biochemical oxygen demand	40 mg/L
Chemical oxygen demand	120 mg/L
pH	5.5–6.5
Total suspended solids	240 mg/L
Electrical conductivity	3–3.5 μmho/cm
Turbidity	4–8 NTU
Temperature	21°C–24°C
Total coliform	500,000
Fecal coliform	4,000

$$E = \frac{C_i - C_f}{C_i} \times 100 \quad (1)$$

where C_i and C_f are the initial and final MPN/100 mL, respectively [7,21].

3. Results and discussion

3.1. Field-emission scanning electron microscopy

The scanning electron microscopy images were utilized to observe the morphology and shape of non-doped and N-doped TiO_2 nanoparticles (Fig. 3). The as-prepared nanoparticles were irregular in shape, forming larger irregular grains by agglomeration, and also, the nanoparticles had a smooth surface. In addition, the particle diameters were approximately 30–40 nm, agreeing with the size of the crystal achieved by the XRD technique. Therefore, the un-doped and N-doped particles are available as nanoparticles.

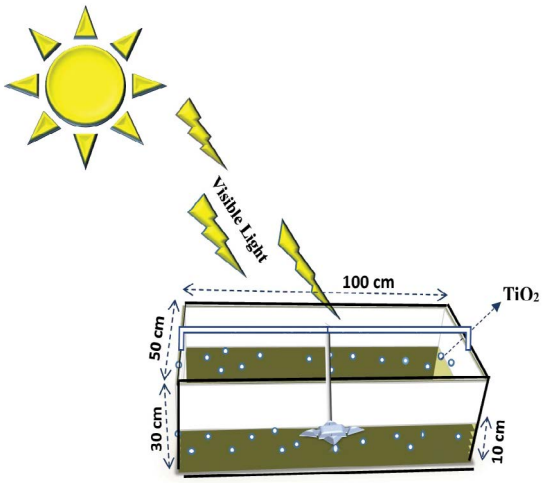

Fig. 2. Schematic of reactor photocatalytic process.

3.2. X-ray of samples

The X-ray diffraction analyses were employed to explore the crystalline material type and evaluate the change after doping N-doped TiO_2. Fig. 4a depicts the XRD diffractograms of non-doped and N-doped TiO_2 nanoparticles. All samples presented sharp diffraction peaks, characteristic of good crystallinity. The XRD peaks, which are observed at 25.49°, 37.14°, 37.99°, 38.76°, 48.35°, 54.12°, 55.33°, 62, 90° and 68.95°, were related to the TiO_2 anatase phase (JCPDF 20-0387). The TiO_2 anatase was the predominant phase for non-doped and N-doped TiO_2 for all the situations utilized.

These results revealed that the 2q diffraction pattern angles were similar for all the samples. No remarkable dopant-related diffraction peaks were obtained in the N-doped TiO_2 samples, indicating that there is no formation of bonds between the nitrogen dopants and TiO_2 to form new crystalline phases. Several papers have also confirmed that doping with the N species has not presented any additional phases with TiO_2 besides anatase.

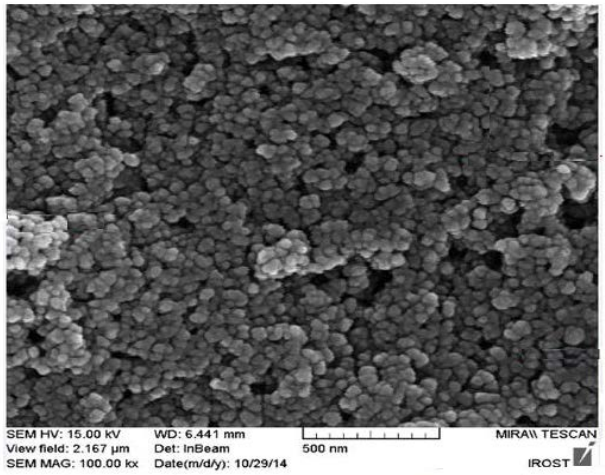

Fig. 3. Field-emission scanning electron microscopy image of synthesis of N-doped TiO_2.

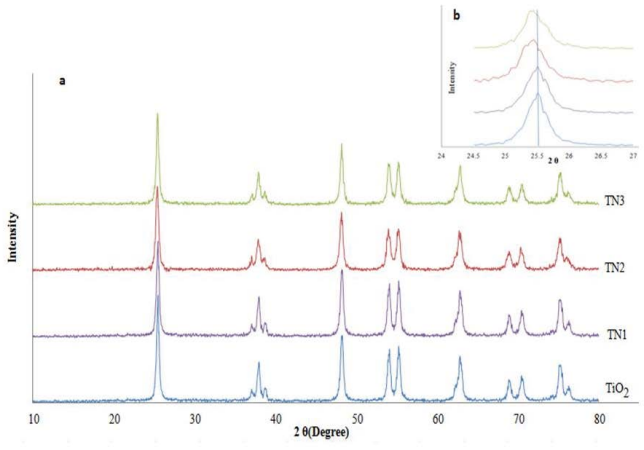

Fig. 4. X-ray diffraction analyses of synthesis of N-doped TiO_2.

The unchanged anatase phase in the N-doped TiO_2 sample can be because the N-dopants are present in low contents, and the N-dopants have dislocated into the substitution sites or interstitial positions of the crystal structure of TiO_2. In addition, the N-doped TiO_2 samples peak presented a small shift toward the lower angle assigned to the (1 0 1) plane of anatase (one of the tetragonal forms of TiO_2, which usually is brown crystals) (Fig. 1b), inferring an N-doped TiO_2 lattice distortion. Therefore, these small particle disorderly states are assigned key factors for absorption edge shift towards the visible-light region caused by nitrogen dopants.

The Debye–Scherrer equation calculated 30, 30, 26, and 34 nm for NT1, NT2, and NT3 un-doped TiO_2 nanoparticles, respectively.

3.3. Effect of visible light irradiation and N-doped TiO_2 nanoparticles

Disinfection experiments were conducted with 180 mg/L N-doped TiO_2 under different situations, including a dark experiment (only photocatalyst) and visible light irradiation in the presence and absence of a photocatalyst. The effect of visible light irradiation and N-doped TiO_2 on the removal of total coliform and fecal coliform bacteria are shown in Fig. 5a and b. The experiments were performed at initial MPN/100 mL 5×10^5 coliform and 4×10^3 MPN/100 mL fecal coliform bacteria's, N-doped TiO_2 dosage 180 mg/L, pH = 7.0 ± 0.5 and retention time 150 min. The results showed that the photocatalytic process is more effective than visible light irradiation for demolishing coliform and fecal coliform bacteria. Also, the demolition efficiency of coliform and fecal coliform bacteria was low over time in the absence of either N-doped TiO_2 or visible light irradiation, while the destruction efficiency was increased in the presence of both N-doped TiO_2 and light irradiation so that after 150 min, total coliforms from 500,000 MPN/100 mL to 7,000 MPN/100 mL and the fecal coliforms from 3,000 MPN/100 mL to 200 MPN/100 mL were reduced. The reason is that in the presence of N-doped TiO_2 and visible light irradiation, hydroxyl radicals ($OH^{\bullet}$) are produced, increasing the efficiency of the photocatalytic process. In the dark condition, the photocatalyst probably adsorbed some of the bacteria, which caused a low reduction in the bacterial population [15]. In the study of Rahmani et al. [15], coliform removal by the photocatalytic method using N-doped TiO_2 was investigated, and they stated that the removal efficiency of coliform in the presence of UV radiation and N-doped TiO_2 nanoparticles alone was less than the TiO_2/UV process. Alikhani et al. [22] in their study reported that the removal efficiency of *Escherichia coli* in the ZnO/UV process was approximately 45%, and it is better than UV alone because of the photocatalytic activity. Different factors, including bacteria population, wastewater composition, and photolyase bacteria, can also contribute as a mechanism in eliminating bacteria [23]. The study's results by Rizzo et al. [24] contrast this study. They observed the highest bacterial inactivation efficiency in the absence of TiO_2 while the wastewater was irradiated using a 250 W UV lamp. Almasi et al. [25] reported that a minimum elimination rate was observed when pH was less than 7.

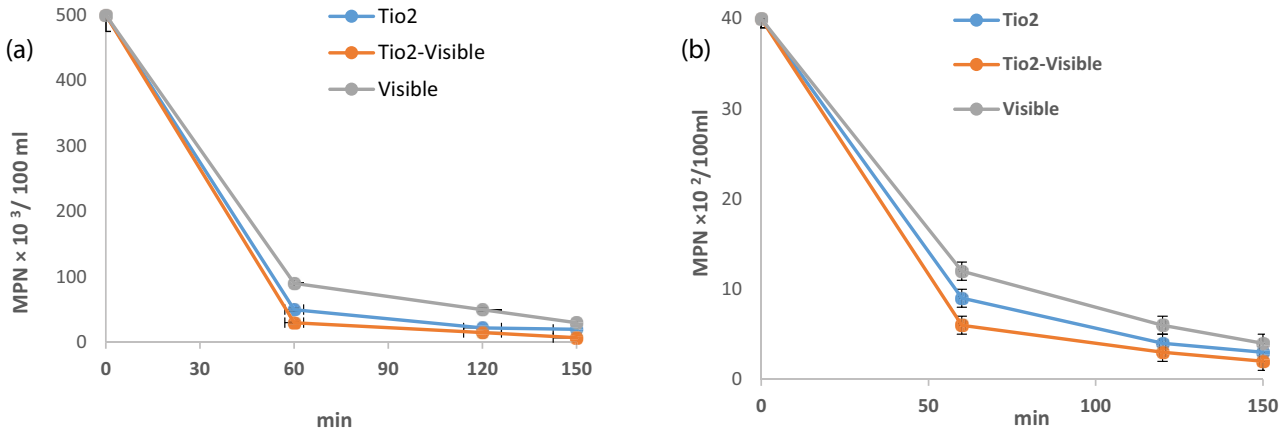

Fig. 5. Effect of irradiation time on coliform (a) and fecal coliform (b) removal: TiO_2 = 180 mg/L, pH = 7.0.

3.4. Bacterial inactivation mechanism

When the photocatalyst is irradiated by sunlight, e^-, h^+ pairs are formed if photons hitting the catalyst have the same or energy over the bandgap N-doped TiO_2 (3.2–3.35 eV). Theoretically, the band gap in semiconductor materials is the void energy region that separates the valence band (VB) from the conduction band (CB). When photons hit the photocatalyst, an electron (e^-) is transferred into the CB and simultaneously creates an h^+ in the VB. Therefore, e^-, h^+ pairs are separated by the energy gap, allowing different redox reactions to form different free radicals at the photocatalyst surface [17]. The produced radicals attack and destroyed the bacterial cells. Catalase, an intracellular enzyme, is an antioxidant that is caused to decompose H_2O_2 into water and oxygen, while superoxide dismutase is an enzyme that decomposes O_2 molecules into H_2O_2 and O_2. They are enzymes that protect bacterial cells from oxidative stress by converting produced radicals into less or non-harmful substances. In this manner, higher levels of superoxide dismutase and catalase can protect bacterial cells from radical attack. It is commonly found that the enzyme-induced levels augment and then decay along with the photocatalytic process. It is shown that the defense capacity of intracellular defense enzymes rapidly increased in the initial stage and then gradually disappeared. However, reducing the superoxide dismutase and catalase activities can accelerate the accumulation of radicals and reduce the viability of the cell. The injury caused by the oxidative stress defense system results in the release of ions, the fragmentation and decomposition of corresponding proteins, and the generation of protein carbonyl derivatives. Finally, bacterial cell collapse occurs. Likewise, other substances and enzymes, such as carotenoid, glutathione, and peroxidase, may also protect the cells of bacteria against radicals [26].

3.5. Effect of contact time and TiO_2 concentration

Catalyst dosage in photocatalytic processes is one of the most important operating parameters affecting free radical production rates and photocatalytic activities. Increasing the photocatalyst dose resulted in a significant decrease in bacterial activity, as shown in Fig. 4. Increasing the synthesized photocatalyst dose from 120 to 180 mg/L increased the removal efficiency from 94.6 to 98/6. However, under the same situation, TiO_2 nanoparticles could increase the removal efficiency from 90% to 92% for fecal coliform. In a study, Shim et al. [13] expressed that by increasing C-N-doped TiO_2 dosage from 0.25 to 1.00 g/L, the bacterial cell inactivation increased from 2.02 to 2.45 log, and a linear relationship was found between N-doped TiO_2 dose and bacterial cell intolerance (R^2 = 0.99). However, a further increase in the photocatalyst dose resulted in a decrease in bacterial elimination, which may be the result of excessive turbidity caused by the high photocatalyst dose, which led to reducing light penetration and $OH^•$ production. Moreover, an excessive increase in photocatalyst leads to the agglomeration of N-doped TiO_2 and reduces the effective surface area of the photocatalyst [27]. The study by Ouyang et al. [28] showed that at low doses, the radiated light could not be fully utilized by the catalyst, resulting in less radical production. However, with increasing the photocatalyst dose, more radiated light can be absorbed to produce more active radicals, which can simultaneously increase soluble turbidity. Also, various studies have shown that increasing the dose of the nanoparticle within a certain range can increase the disinfection efficiency of effluent, but increasing the dose of the nanoparticle up to the optimum can lead to agglomeration of the catalyst, creating turbidity and reducing the penetration of light into the media, which is led to reducing disinfection efficiency [29].

Moreover, Fig. 6 shows that the removal of total coliform and fecal coliform under photocatalyst is affected by the contact time, such that increasing the contact time could improve the disinfection rate. The result of the study conducted by Kiwi et al. [30] showed that in solar water disinfection for all systems (untreated bottles, half black bottles, and half N-doped TiO_2 thin bottles), the number of bacteria gradually decreased by increasing the contact time.

At first, the intact bacterial cell walls are observed, and TiO_2 particles are positioned at a distance in the cell wall based on the theory of colloidal stability. The attractive Van der Waals forces lead to the aggregate of N-doped TiO_2 within 30 min. Then, TiO_2 aggregated approximately accumulates at the cell wall surface and can damage the cell wall

in the contact area between the TiO_2 and the bacteria due to strong adsorption between the neutral charge TiO_2 and the cell wall.

Ultimately, in some areas of the sample, the outer layers of the cell wall become discontinuous; in others, the cell wall disappears. Damage to the cell wall results in the inactivation of cells, including changes in cell morphology and bacterial activity [30].

3.6. Kinetic modeling

In order to study kinetic reaction, first-order kinetic was used for modeling the data [Eq. (2)].

$$\ln\left(\frac{N_0}{N_t}\right) = k_0 t \tag{2}$$

where N_0, N_t, and k_0, t are the numbers of primary cells at the initial time, the number of living cells at the time of t, and the pseudo-first-order reaction rate constant (min^{-1}) and reaction time (min), respectively. The reaction rate constant (k_0) can be calculated from the slope of a plot of L_n (N_0/N_t) vs. (t). The results of the kinetic reaction for the total coliform and fecal coliform were plotted in Fig. 7a and b by first-order modeling. This study evaluated the effect of different disinfection systems, including visible light, N-doped TiO_2, and TiO_2/visible light, on the inactivation rate of fecal coliform and fecal coliform. The values of the disinfection rate constant (k) in different states and their determination coefficients (R^2) are indicated in Table 2.

The result showed that the lowest and highest reaction constant for total coliform is related to visible light alone (1.79×10^{-2}) and N-doped TiO_2/visible light system (2.8×10^{-2}), respectively. The same results were obtained for fecal coliform such that the lowest and highest reaction constant was

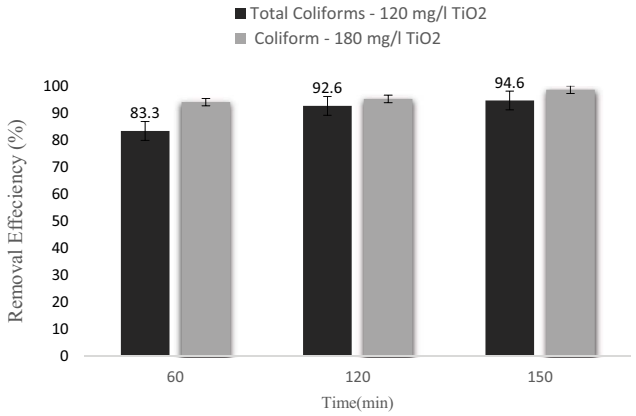

Fig. 6. Effect of N-doped TiO_2 dosage on total coliform and fecal coliform removal at different times.

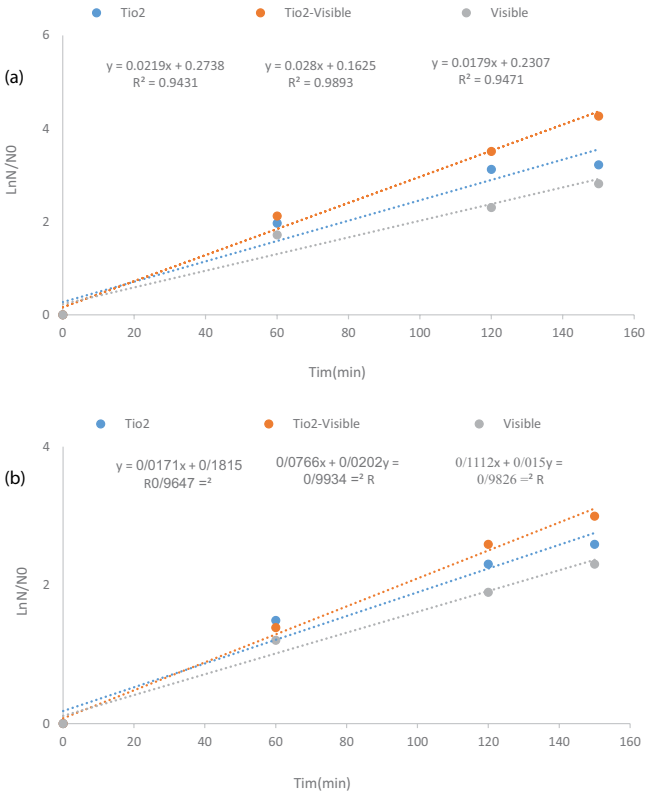

Fig. 7. Reaction kinetics of total coliform (a) and fecal coliform (b).

Table 2
Results of modeling of experimental kinetic data of different disinfection systems on coliform and fecal coliform inactivation

Microorganism	Parameter	Value	Equation	k_0 (min^{-1})	R^2	$t_{1/2}$ (min)*
Total coliform	Disinfection process	Visible	$y = 0/0179x + 0/2,307$	1.79×10^{-2}	0.9893	38.71
		TiO_2	$y = 0/0219x + 0/2,738$	2.19×10^{-2}	0.9431	31.64
		Vis/TiO_2	$y = 0/028x + 0/1,625$	2.8×10^{-2}	0.9471	24.75
N-doped	TiO_2 concentration	120	$y = 0/0191x + 0/2,464$	1.91×10^{-2}	0/949	36.28
		180	$y = 0/0252x + 0/4,349$	2.52×10^{-2}	0/8825	27.5
Fecal coliform		Visible	$y = 0/015x + 0/1,112$	0.15×10^{-2}	0.9826	46.2
		TiO_2	$y = 0/0171x + 0/1,815$	1.71×10^{-2}	0.9647	40.52
		Vis/TiO_2	$y = 0/0202x + 0/0766$	2.02×10^{-2}	0.9934	34.30
		120	$y = 0/0193x + 0/2,757$	1.93×10^{-2}	0/8705	35.90
		180	$y = 0/0268x + 0/4,327$	2.68×10^{-2}	0/9713	25.8

related to visible light alone (0.15×10^{-2}) and N-doped TiO_2/visible light system (2.68×10^{-2}), respectively.

Fig. 7a and b show that only 3.2% of the coliforms population and 2.6% of the fecal coliforms population remained in the N-doped TiO_2/visible light system by regression coefficients of 0.94 and 0.96, respectively. Generally, the results show that visible light and TiO_2 alone have poor disinfection capabilities, such that the simultaneous use of N-doped TiO_2 and visible light in an integrated system can significantly increase the constant rate of disinfection. Finally, it can be found that the kinetic data from the disinfection of coliform and fecal coliform under visible light/N-doped TiO_2 process followed the first-order equation by regression coefficients of 0.94 and 0.99, respectively.

4. Conclusion

In this study, when the synthesized N-doped TiO_2 nanoparticles were characterized and confirmed by FE-SEM and XRD analysis, the photocatalytic process using N-doped TiO_2 nanoparticles under solar irradiation was used to disinfect and eliminate coliform and fecal coliform bacteria from treatment plant effluent of hospital wastewater. The results expressed that the disinfection process's efficiency was affected by the bacterial type, nanoparticles dose, and visible light. Further, the result showed that the efficiency of the visible light/N-doped TiO_2 process for bacteria elimination from effluent was more than visible light and N-doped TiO_2 alone. At high disinfection time (150 min), the removal values of coliform and fecal coliform were 98.6% and 92%, respectively. The photocatalytic activity by visible light/N-doped TiO_2 system is an inexpensive, economical, and affordable technic, although this process needs a long time to disinfect the real effluent due to sunlight.

Acknowledgment

The authors thank Zahedan University of Medical Sciences for supporting this article with ethics and project codes IR, ZAUMS.REC.1397.145 and 8883 respectively. Also, the authors would like to thank Professor Eder C. Lima for improving English language of this paper.

Funding

The paper was supported by Zahedan University of Medical Sciences.

References

[1] J. Rodríguez-Chueca, S. Mesones, J. Marugán, Hybrid UV-C/microfiltration process in membrane photoreactor for wastewater disinfection, Environ. Sci. Pollut. Res., 26 (2019) 36080–36087.
[2] M.T. Moustafa, Removal of pathogenic bacteria from wastewater using silver nanoparticles synthesized by two fungal species, Water Sci., 31 (2017) 164–176.
[3] D.T. Sponza, P. Alicanoglu, Reuse and recovery of raw hospital wastewater containing ofloxacin after photocatalytic treatment with nanographene oxide magnetite, Water Sci. Technol., 77 (2017) 304–322.
[4] P.R. Maddigpu, B. Sawant, S. Wanjari, M.D. Goel, D. Vione, R.S. Dhodapkar, S. Rayalu, Carbon nanoparticles for solar disinfection of water, J. Hazard. Mater., 343 (2018) 157–165.
[5] A. Hossein Panahi, A. Meshkinian, S.D. Ashrafi, M. Khan, A. Naghizadeh, G. Abi, H. Kamani, Survey of sono-activated persulfate process for treatment of real dairy wastewater, Int. J. Environ. Sci. Technol., 17 (2020) 93–98.
[6] F.S. Arghavan, T.J. Al-Musawi, E. Allahyari, M.H. Moslehi, N. Nasseh, A. Hossein Panahi, Complete degradation of tamoxifen using $FeNi_3$@SiO_2@ZnO as a photocatalyst with UV light irradiation: a study on the degradation process and sensitivity analysis using ANN tool, Mater. Sci. Semicond. Process., 128 (2021) 105725, doi: 10.1016/j.mssp.2021.105725.
[7] F.S. Arghavan, A. Hossein Panahi, N. Nasseh, M. Ghadirian, Adsorption-photocatalytic processes for removal of pentachlorophenol contaminant using $FeNi_3$/SiO_2/ZnO magnetic nanocomposite under simulated solar light irradiation, Environ. Sci. Pollut. Res., 28 (2021) 7462–7475.
[8] E. Norabadi, A.H. Panahi, R. Ghanbari, A. Meshkinian, H. Kamani, S.D. Ashrafi, Optimizing the parameters of amoxicillin removal in a photocatalysis/ozonation process using Box–Behnken response surface methodology, Desal. Water Treat., 192 (2020) 234–240.
[9] M.R. Delsouz Khaki, M.S. Shafeeyan, A.A.A. Raman, W.M.A.W. Daud, Evaluating the efficiency of nano-sized Cu doped TiO_2/ZnO photocatalyst under visible light irradiation, J. Mol. Liq., 258 (2018) 354–365.
[10] S. Masoomeh Rahimi, A. Hossein Panahi, N. Sadat Mazari Moghaddam, E. Allahyari, N. Nasseh, Breaking down of low-biodegradation Acid Red 206 dye using bentonite/Fe_3O_4/ZnO magnetic nanocomposite as a novel photo-catalyst in presence of UV light, Chem. Phys. Lett., 794 (2022) 139480, doi: 10.1016/j.cplett.2022.139480.
[11] N. Nasseh, M.T. Samadi, M. Ghadirian, A. Hossein Panahi, A. Rezaie, Photo-catalytic degradation of tamoxifen by using a novel synthesized magnetic nanocomposite of $FeCl_2$@ac@ZnO: a study on the pathway, modeling, and sensitivity analysis using artificial neural network (AAN), J. Environ. Chem. Eng., 10 (2022) 107450, doi: 10.1016/j.jece.2022.107450.
[12] Q. Li, S. Mahendra, D.Y. Lyon, L. Brunet, M.V. Liga, D. Li, P.J.J. Alvarez, Antimicrobial nanomaterials for water disinfection and microbial control: potential applications and implications, Water Res., 42 (2008) 4591–4602.
[13] J. Shim, Y.-S. Seo, B.-T. Oh, M. Cho, Microbial inactivation kinetics and mechanisms of carbon-doped TiO_2 (C-TiO_2) under visible light, J. Hazard. Mater., 306 (2016) 133–139.
[14] H. Kamani, S.D. Ashrafi, A. Jahantiq, E. Norabadi, M. Dashti Zadeh, Catalytic degradation of humic acid using Fe-doped TiO_2-ultrasound hybrid system from aqueous solution, Int. J. Environ. Anal. Chem., (2021) 1–15, doi: 10.1080/03067319.2021.1979535.
[15] A. Rahmani, M. Samarghandi, M. Samadi, F. Nazemi, Photocatalytic disinfection of coliform bacteria using UV/TiO_2, J. Res. Health Sci., 9 (2009) 1–6.
[16] H. Kamani, S. Nasseri, R. Nabizadeh, M. Khoobi, D. Ashrafi, E. Bazrafshan, A.H. Mahvi, Sonocatalytic oxidation of Reactive Blue 29 by N-doped TiO_2 from aqueous solution, J. Mazandaran Univ. Med. Sci., 28 (2018) 157–169.
[17] D. Venieri, F. Tournas, I. Gounaki, V. Binas, A. Zachopoulos, G. Kiriakidis, D. Mantzavinos, Inactivation of *Staphylococcus aureus* in water by means of solar photocatalysis using metal doped TiO_2 semiconductors, J. Chem. Technol. Biotechnol., 92 (2017) 43–51.
[18] H. Kamani, S. Nasseri, M. Khoobi, R. Nabizadeh Nodehi, A.H. Mahvi, Sonocatalytic degradation of humic acid by N-doped TiO_2 nano-particle in aqueous solution, J. Environ. Health Sci. Eng., 14 (2016) 3, doi: 10.1186/s40201-016-0242-2.
[19] A. Jahantiq, R. Ghanbari, A. Hossein Panahi, S.D. Ashraf, A.D. Khatibi, Photocatalytic degradation of 2,4,6-trichlorophenol in aqueous solutions using synthesized Fe-doped TiO_2 nanoparticles via response surface methodology, Desal. Water Treat., 183 (2020) 366–373.
[20] W.E. Federation, A. Association, Standard Methods for the Examination of Water and Wastewater, American Public Health Association (APHA), Washington, D.C., USA, 2005.

[21] N. Nasseh, F.S. Arghavan, S. Rodriguez-Couto, A. Hossein Panahi, Synthesis of $FeNi_3/SiO_2/CuS$ magnetic nano-composite as a novel adsorbent for Congo Red dye removal, Int. J. Environ. Anal. Chem., 102 (2022) 2342–2362.
[22] M.-Y. Alikhani, S.-M. Lee, J.-K. Yang, M. Shirzad-Siboni, H. Peeri-Dogaheh, M.-S. Khorasani, M.-A. Nooshak, M.-R. Samarghandi, Photocatalytic removal of *Escherichia coli* from aquatic solutions using synthesized ZnO nanoparticles: a kinetic study, Water Sci. Technol., 67 (2013) 557–563.
[23] A.P.H. Association, A.W.W. Association, W.P.C. Federation, W.E. Federation, Standard Methods for the Examination of Water and Wastewater, American Public Health Association, 1912.
[24] L. Rizzo, A. Della Sala, A. Fiorentino, G. Li Puma, Disinfection of urban wastewater by solar driven and UV lamp – TiO_2 photocatalysis: effect on a multi-drug resistant *Escherichia coli* strain, Water Res., 53 (2014) 145–152.
[25] A. Almasi, M. Mohammadi, A. Dargahi, N. Bahmani, The effect of visible light on microbial load decrease in facultative stabilization ponds, Int. J. Occup. Environ. Health., 3 (2017) 20–27.
[26] W. Wang, G. Huang, J.C. Yu, P.K. Wong, Advances in photocatalytic disinfection of bacteria: development of photocatalysts and mechanisms, J. Environ. Sci., 34 (2015) 232–247.
[27] M. Pratap Reddy, H.H. Phil, M. Subrahmanyam, Photocatalytic disinfection of *Escherichia coli* over titanium(IV) oxide supported on Hβ zeolite, Catal. Lett., 123 (2008) 56–64.
[28] K. Ouyang, K. Dai, S.L. Walker, Q. Huang, X. Yin, P. Cai, Efficient photocatalytic disinfection of *Escherichia coli* O157:H7 using C 70-TiO_2 hybrid under visible light irradiation, Sci. Rep., 6 (2016) 1–8.
[29] M. Ahmadi, M.-J. Mohammadi, K. Ahmadi-Angaly, A.-A. Babaei, Failures analysis of water distribution network during 2006–2008 in Ahvaz, Iran, J. Adv. Environ. Health Res., 1 (2013) 129–137.
[30] J. Kiwi, S. Rtimi, R. Sanjines, C. Pulgarin, TiO_2 and TiO_2-doped films able to kill bacteria by contact: new evidence for the dynamics of bacterial inactivation in the dark and under light irradiation, Int. J. Photoenergy, 2014 (2014) 785037, doi: 10.1155/2014/785037.